EFFECT OF LINEAR AND NON-LINEAR GEOPHONE ARRAYS ON SIGNAL-TO-NOISE RATIO OF SEISMIC REFLECTION DATA

IONELIA PANEA, IONUȚ ZGORCEA

University of Bucharest, Faculty of Geology and Geophysics, Department of Geophysics, 6, Traian Vuia St., 020956, Bucharest, Romania, ipanea2@yahoo.com

We used linear and non-linear geophone arrays to attenuate the coherent noise seen on single-sensor data recorded in a seismic reflection project performed in the Dumitreşti area, Romania. We compared the responses of linear geophone arrays with 12 elements with those of non-linear geophone arrays (rectangular, circular, cross and fishbone patterns). We showed that the non-linear arrays with circular, cross and fishbone patterns perform the lowest coherent noise attenuattion.

Key words: surface wave, coherent noise, geophone arrays, data acquisition, seismic modeling.

INTRODUCTION

Land seismic reflection data contain coherent noise (surface waves) which can be strongly affected by spatial aliasing, depending on the near-surface conditions and data aquisition parameters. The spatially aliased energy affects the accuracy of the filtering and migration results. This coherent noise can be attenuated during data acquisition using hard-wired geophone arrays directly in the field or computing the array responses using seismic data from single-sensor measurements before the data processing (Panea, Drijkoningen, 2008). Panea (2009) showed that the use of hard-wired arrays in areas with rough topography and variations in the near-surface conditions can destroy the signal wavelet with effects on the velocity and amplitude analysis.

DESIGNING OF THE LINEAR AND NON-LINEAR GEOPHONE ARRAYS

We display in Figure 1a, a linear geophone array with 12 elements. In our analysis, the group interval, Δx_G, is equal to $2\Delta x_g$, where Δx_g is the spacing between the array elements on the inline and crossline direction. The group interval represents the distance between the centers of two consecutive geophone arrays; it is chosen such that the reflected waves will not be spatially aliased after array forming. The non-linear geophone arrays are displayed in Figures 1b–e. We designed these arrays based on the pattern used in the field for single-sensor seismic measurements.

We used all five arrays on a synthetic single-sensor record to analyze and compare the surface wave attenuation produced by each of this array. The single-sensor record was modeled for a horizontally layered medium; the thickness of the first layer was 200 m. The surface wave is characterized by a frequency of 12 Hz and an apparent velocity of 450 m/s. The reflected wave is characterized by a frequency of 36 Hz and an apparent velocity of 1700 m/s. The Ricker wavelet was used in modeling. A number of 80 geophones spaced at 5 m were used to obtain the synthetic record on which we used linear arrays. A single-sensor record with 5 × 80 geophones spaced at 5 m on inline and crossline directions was modeled for the use of non-linear arrays. The time sampling interval was 0.001 s. The trace length was 0.5 s.

We display in Figures 2–4 the responses of the linear arrays computed for the traces 1–12, 19–30 and 61–72 selected from the synthetic single-sensor record. A good surface wave attenuation represented by the remaining wavelets seen between 0–0.2 s. For the trace interval 19–30, linear array attenuated well the surface waves and enhanced the reflected wave (compare Figures 3b and 3c). Single-sensor traces 61–70 contain seismic waves coming from great offsets, meaning that the moveout is important in case of the reflected wave (Figure 4a). Array-forming applied on these traces will attenuate both, surface and reflected waves (Figures 4b and 4c). In the presence of significant moveout values, one way to protect the amplitude and shape of the reflected waves is to apply time corrections before array forming (Panea, Drijkoningen, 2006).

Similar surface wave attenuation was seen on the responses of the rectangular array computed for traces 1–12, 19–30 and 61–72 selected on each crossline (Figs. 5–7). The total number of single-sensor traces involved in a rectangular array is 60 (5 × 12).

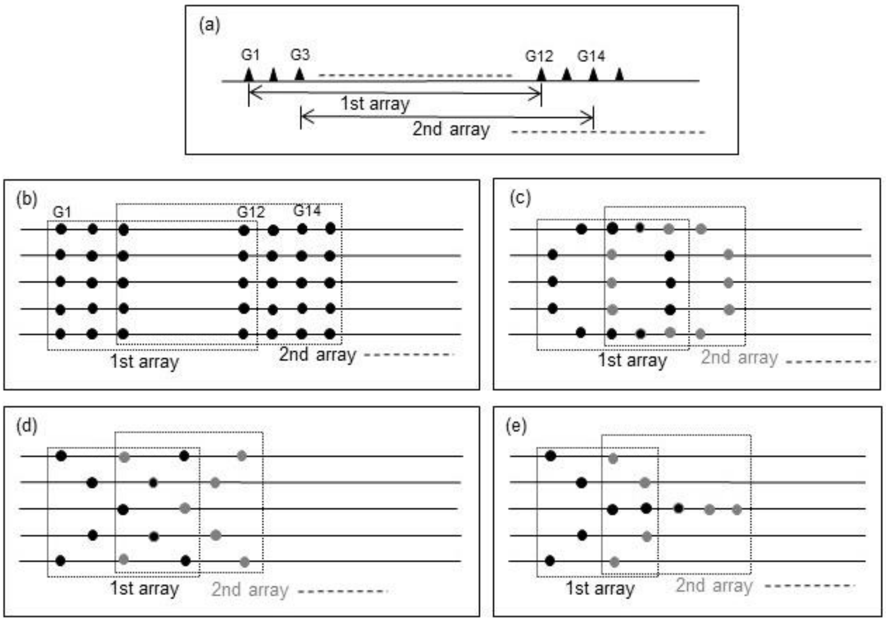

Fig. 1 – (a) Linear and (b-e) non-linear geophone arrays.

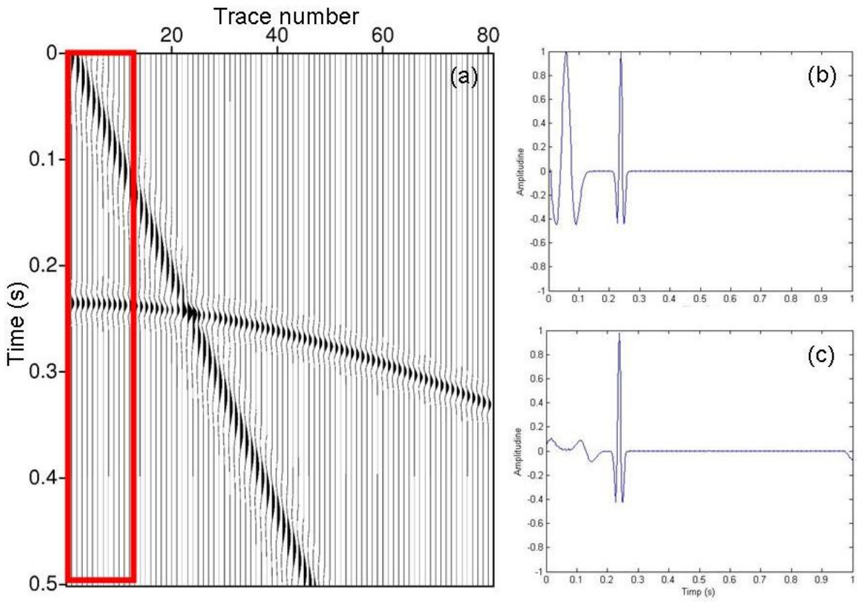

Fig. 2 – (a) Single-sensor traces, 1–12, used in linear array-forming, (b) corresponding single-sensor trace to (c) array response.

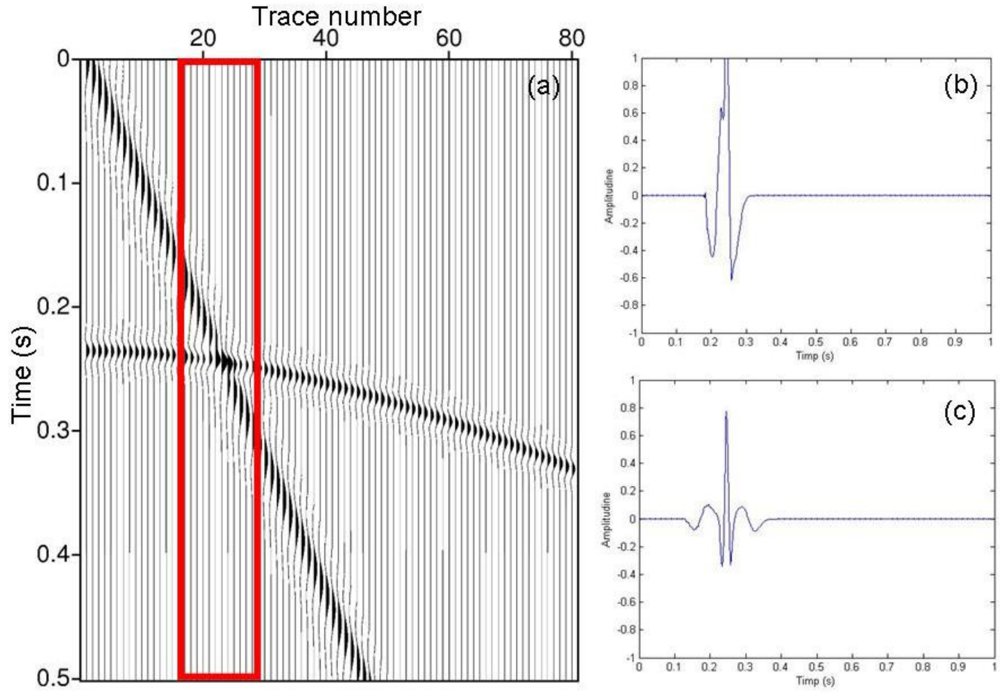

Fig. 3 – (a) Single-sensor traces, 19–30, used in linear array-forming, (b) corresponding single-sensor trace to (c) array response.

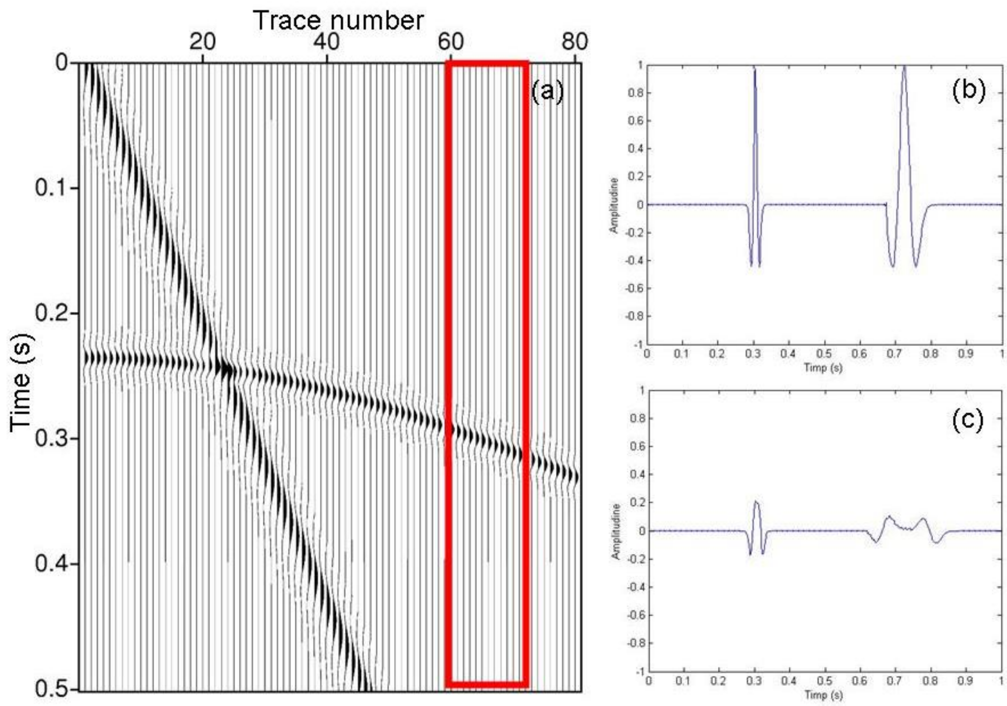

Fig. 4 – (a) Single-sensor traces, 61–72, used in linear array-forming, (b) corresponding single-sensor trace to (c) array response.

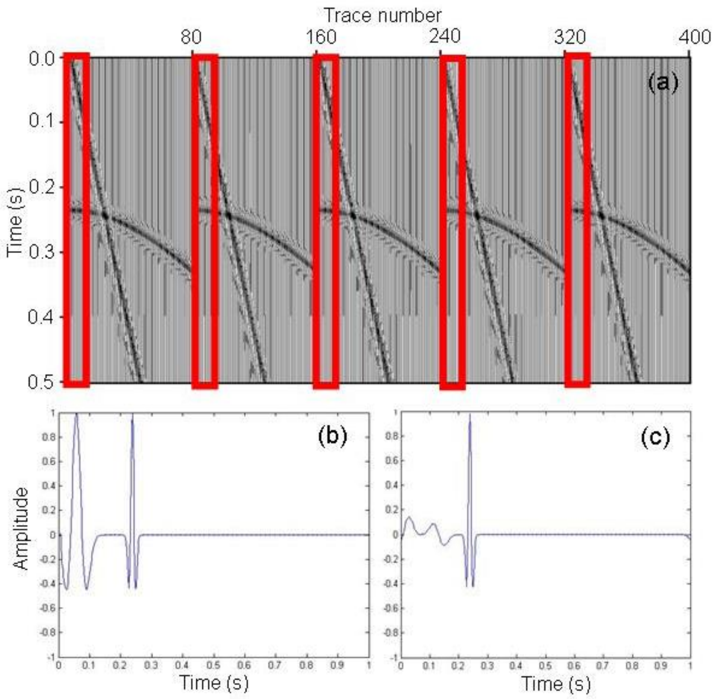

Fig. 5 – (a) Single-sensor traces, 1–12 selected from each line, used in rectangular array-forming, (b) corresponding single-sensor trace to (c) array response.

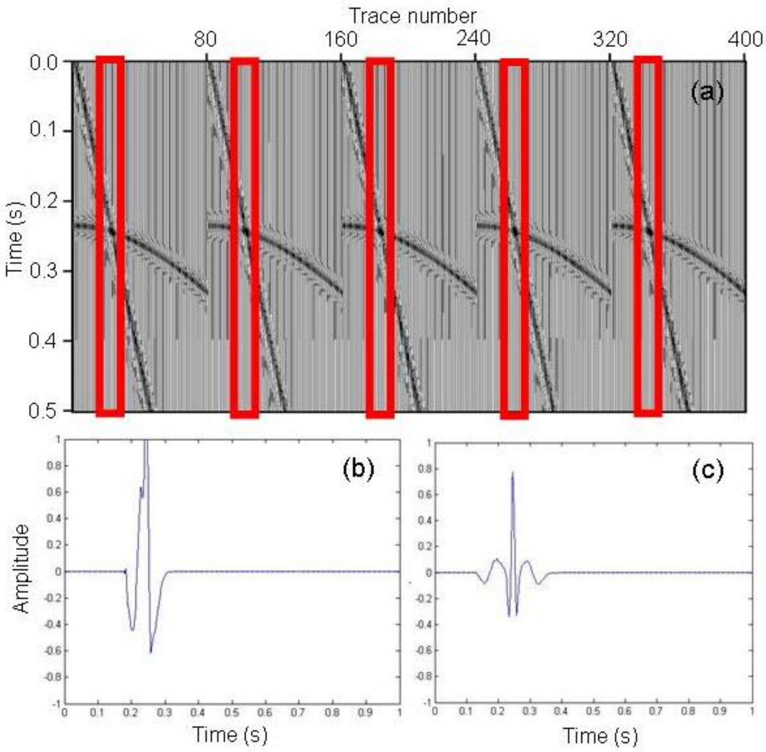

Fig. 6 – (a) Single-sensor traces, 19–30 selected from each line, used in rectangular array-forming, (b) corresponding single-sensor trace to (c) array response.

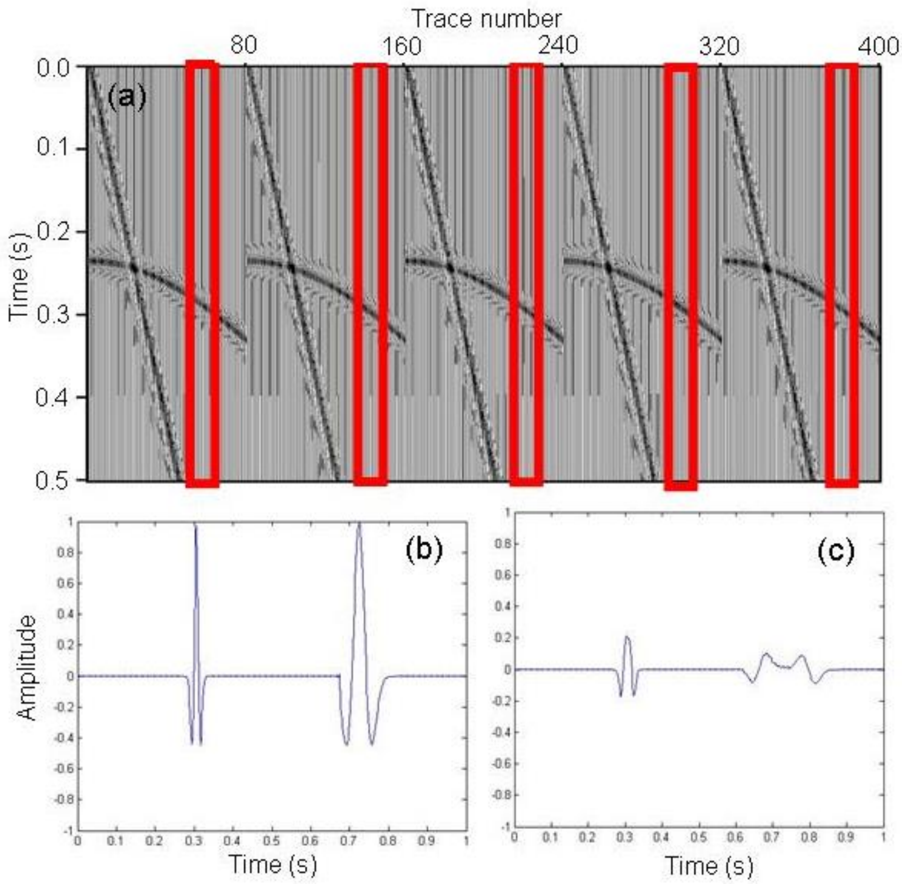

Fig. 7 – (a) Single-sensor traces, 61–72 selected from each line, used in rectangular array-forming, (b) corresponding single-sensor trace to (c) array response.

The circular array-responses obtained for traces which correspond in position with those used for linear and rectangular arrays are displayed in Figures 8–10. By comparing the traces before and after array forming, we notice that the surface wave amplitude is almost identical. The circular array has 12 elements.

In case of the cross array, the surface wave attenuation depends on the position of the traces selected from the single-sensor record. For example, good surface wave attenuation is observed in Figure 12 and low surface wave attenuation is observed in Figures 11 and 13. In case of the fishbone array, we notice a good surface wave attenuation in Figure 15 and a low attenuation in Figures 14 and 16. In all arrays in which the reflected waves from the single-sensor traces show significant moveout, their amplitude is attenuated after array forming (Figures 4, 7, 10, 13 and 16). In these examples, the cross array has 9 elements and the fishbone array has 7 elements.

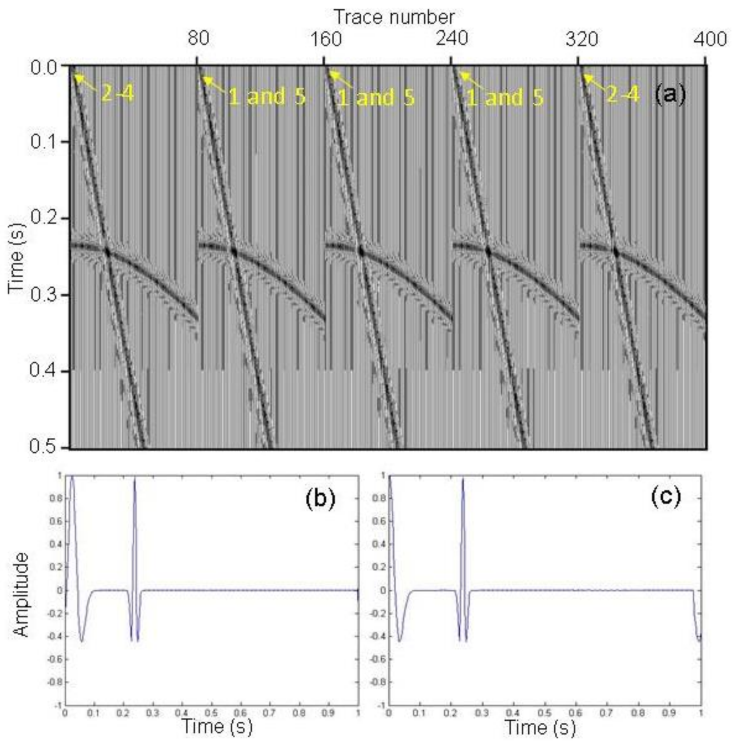

Fig. 8 – (a) Single-sensor traces (yellow) used in circular array-forming, (b) corresponding single-sensor trace to (c) array response.

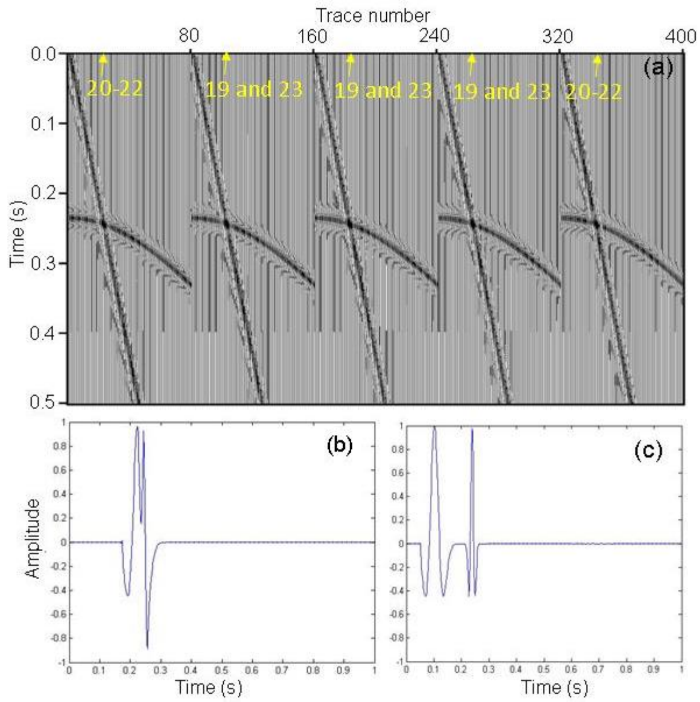

Fig. 9 – (a) Single-sensor traces (yellow) used in circular array-forming, (b) corresponding single-sensor trace to (c) array response.

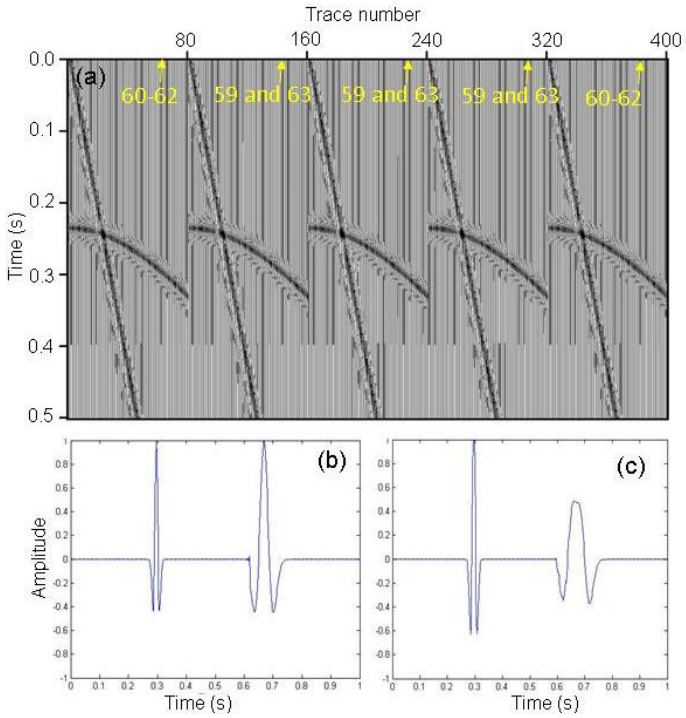

Fig. 10 – (a) Single-sensor traces (yellow) used in circular array-forming, (b) corresponding single-sensor trace to (c) array response.

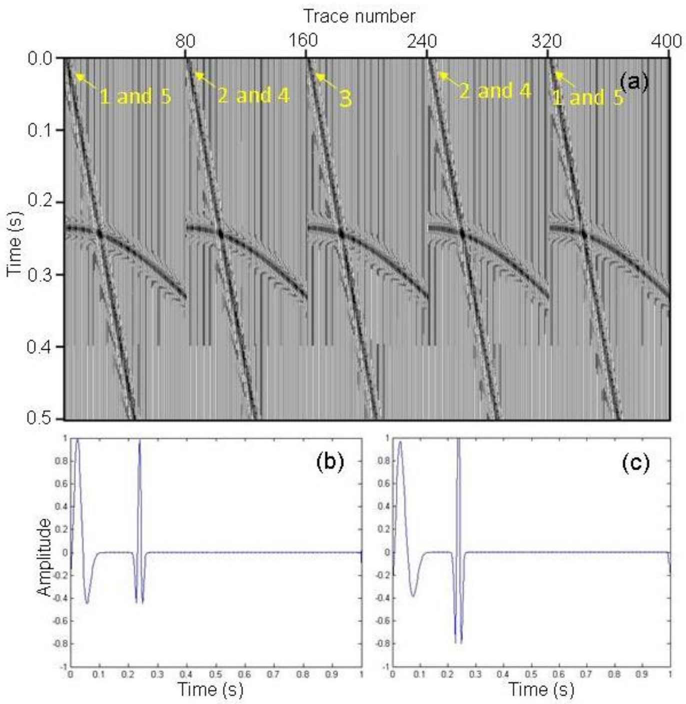

Fig. 11 – (a) Single-sensor traces (yellow) used in cross array-forming, (b) corresponding single-sensor trace to (c) array response.

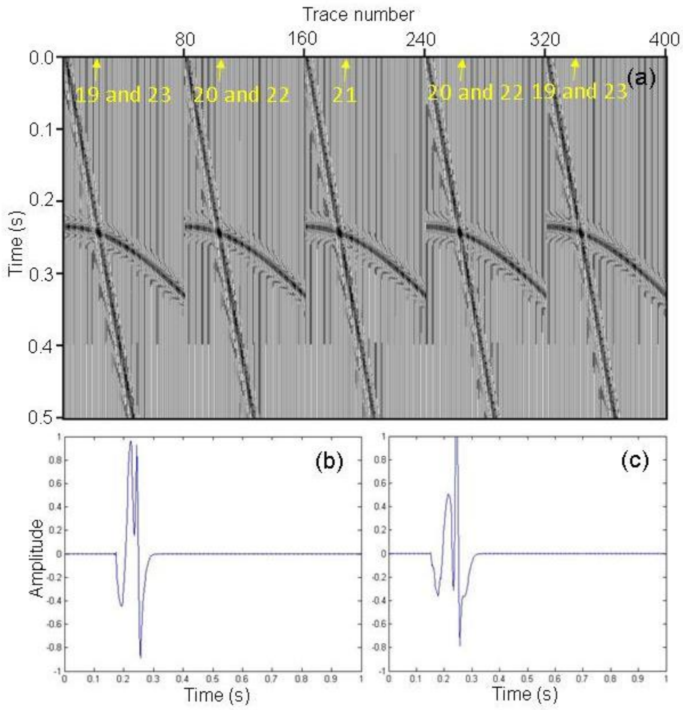

Fig. 12 – (a) Single-sensor traces (yellow) used in cross array-forming,
(b) corresponding single-sensor trace to (c) array response.

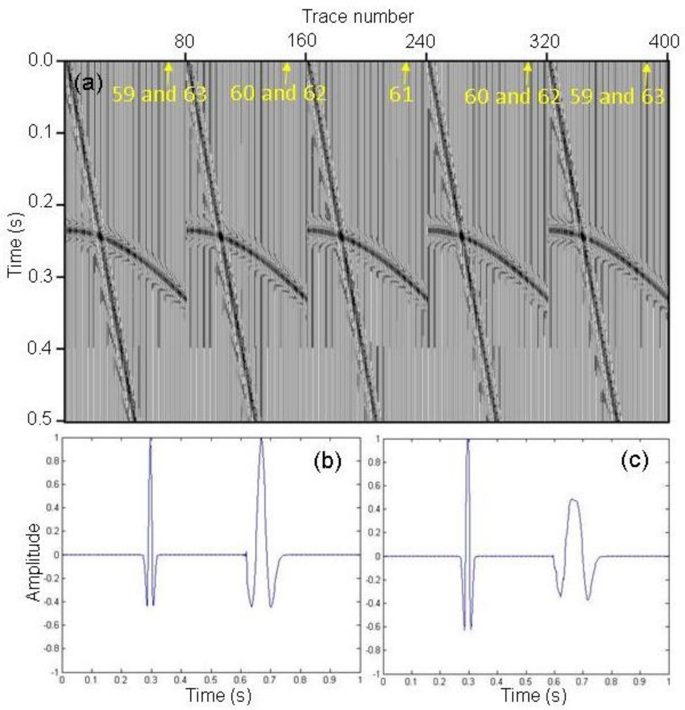

Fig. 13 – (a) Single-sensor traces (yellow) used in cross array-forming,
(b) corresponding single-sensor trace to (c) array response.

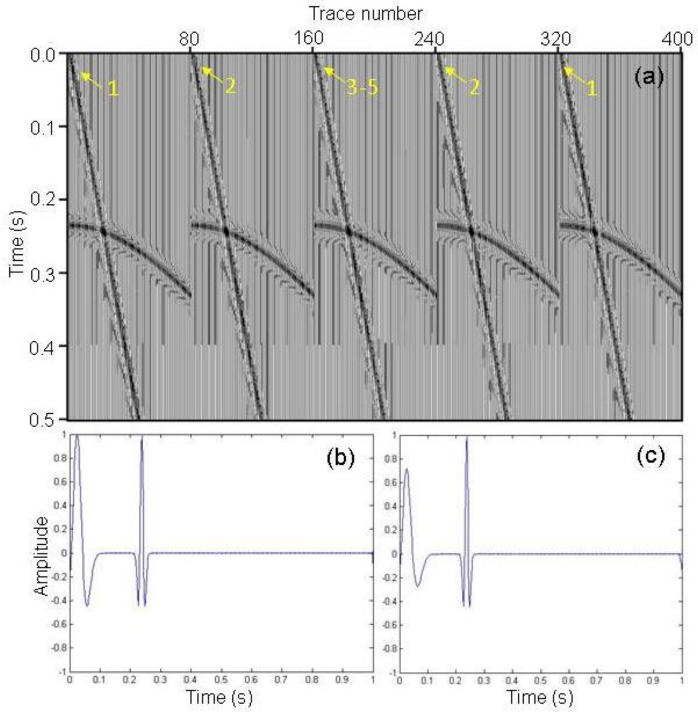

Fig. 14 – (a) Single-sensor traces (yellow) used in fishbone array-forming, (b) corresponding single-sensor trace to (c) array response.

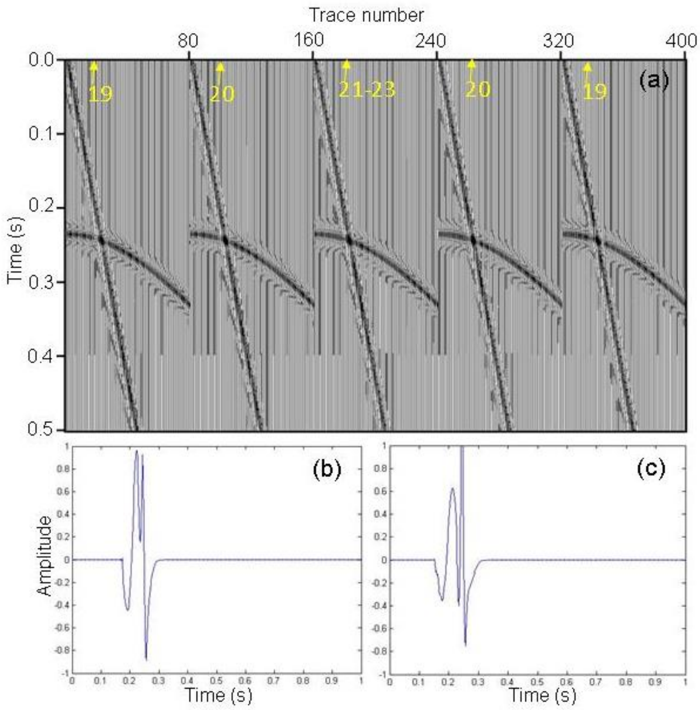

Fig. 15 – (a) Single-sensor traces (yellow) used in fishbone array-forming, (b) corresponding single-sensor trace to (c) array response.

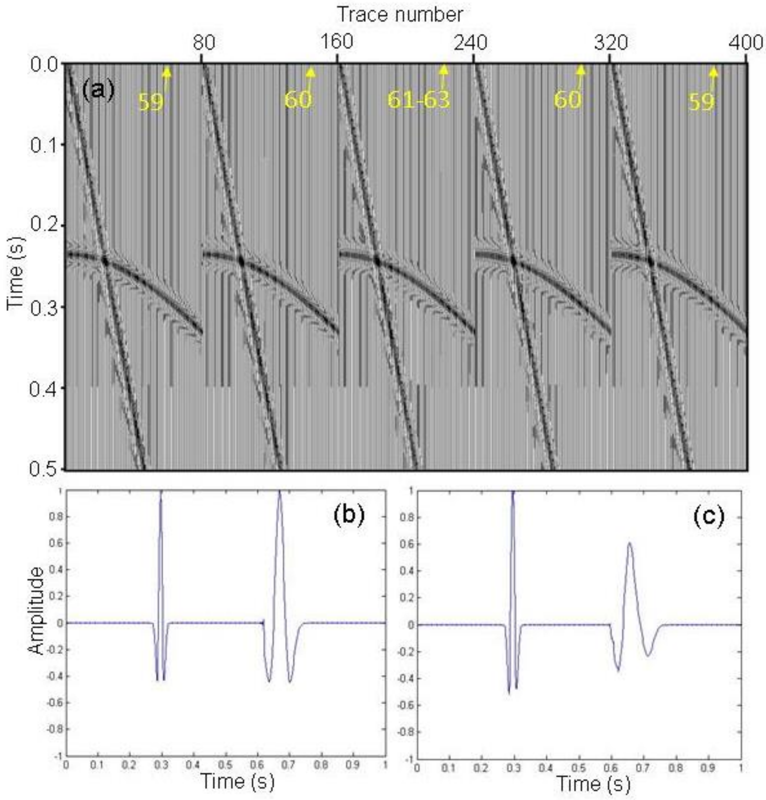

Fig. 16 – (a) Single-sensor traces (yellow) used in fishbone array-forming, (b) corresponding single-sensor trace to (c) array response.

DESCRIPTION OF THE SINGLE-SENSOR SEISMIC DATA

In our analysis, we used single-sensor seismic data recorded in the Dumitreşti area, Romania, in an international research project performed to obtain information about the geological structure of the subsurface (Figure 17). The data acuisition was performed using a strip of five lines with receivers spaced at 5 m on both directions, inline and crossline. Each receiver was represented by 12 vertical-component geophones planted in a rectangular nest (4×3 geophones). The variations in elevations were important along the seismic line (Fig. 17). The maximum number of receivers/ record was 160. The seismic energy was generated using explosive sources (dynamite) in points spaced at 20 m and placed only along the third line. The time sampling interval was 0.001 s. The maximum length of recordings was 4 s.

An example of raw field single-sensor record is displayed in Figure 18a. Trace spacing is 5 m. The surface waves cover the reflected waves at small offsets; they show strong energy in the (f, k)-domain (Figure 18b). All array responses presented below were computed in two steps. First, we added the selected single-sensor traces and, then, we spatially sampled the summation result to the group interval of 10 m. The linear array responses were computed using arrays with 12 elements. The surface wave attenuation is clear on the (t, x)- and (f, k)-domains (Figures 19a,b). Good surface wave attenuation was performed by the rectangular array with 12×5 elements (Figures 20a,b). As expected, based on the results on the synthetic single-sensor data, lower surface wave attenuation was observed after array forming with circular, cross and fishbone patterns (Figures 21a,b, 22a,b and 23a,b).

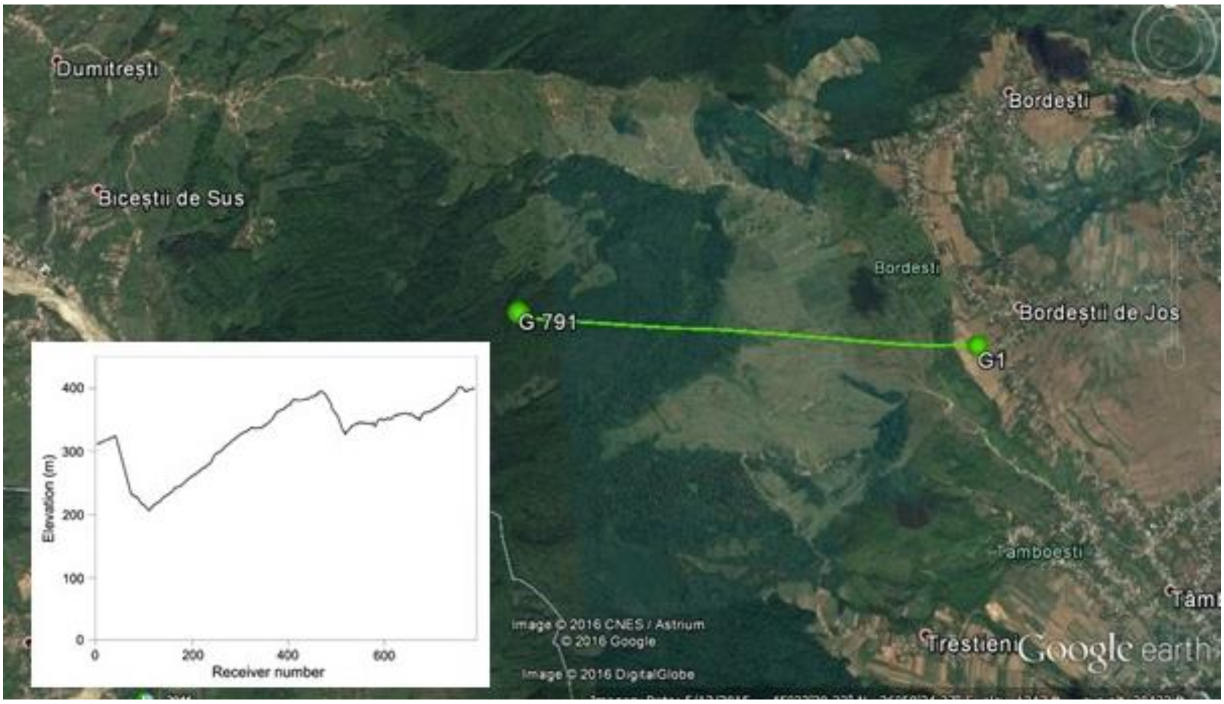

Fig. 17 – Topographic map for the Dumitrești area, Romania, showing the seismic line (green line); inset: elevation variations along the line. Source map: http://maps.google.com.

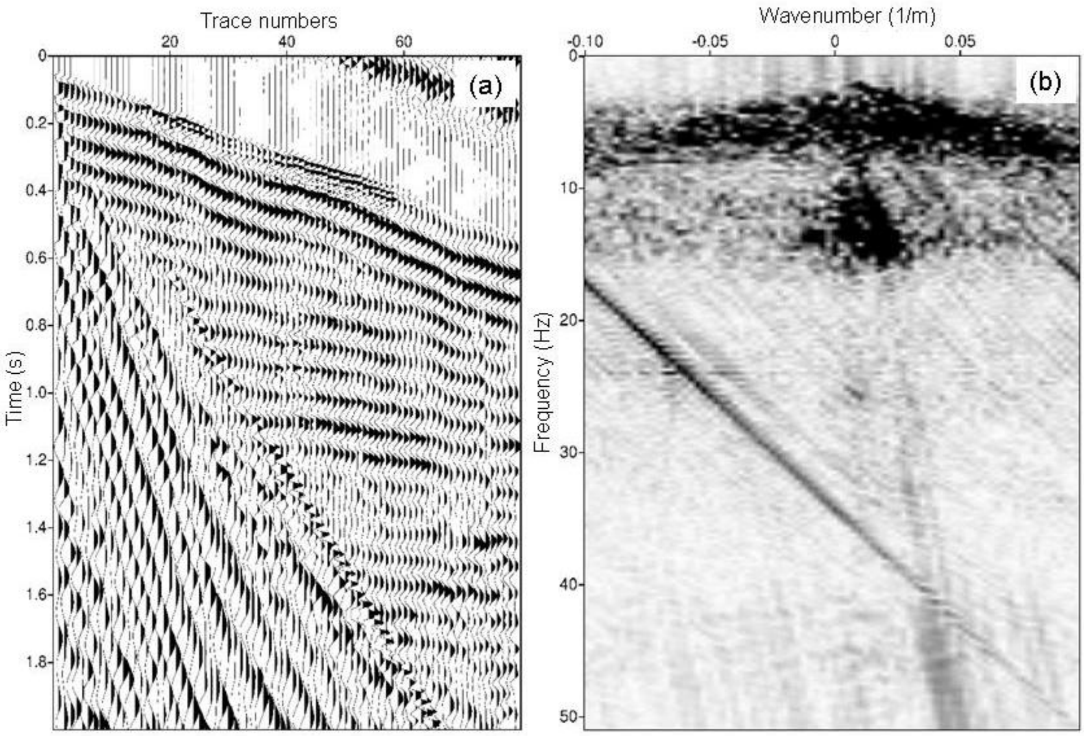

Fig. 18 – Example of field record, trace spacing of 5 m, displayed in time (a) time and (b) frequency-wavenumber domain.

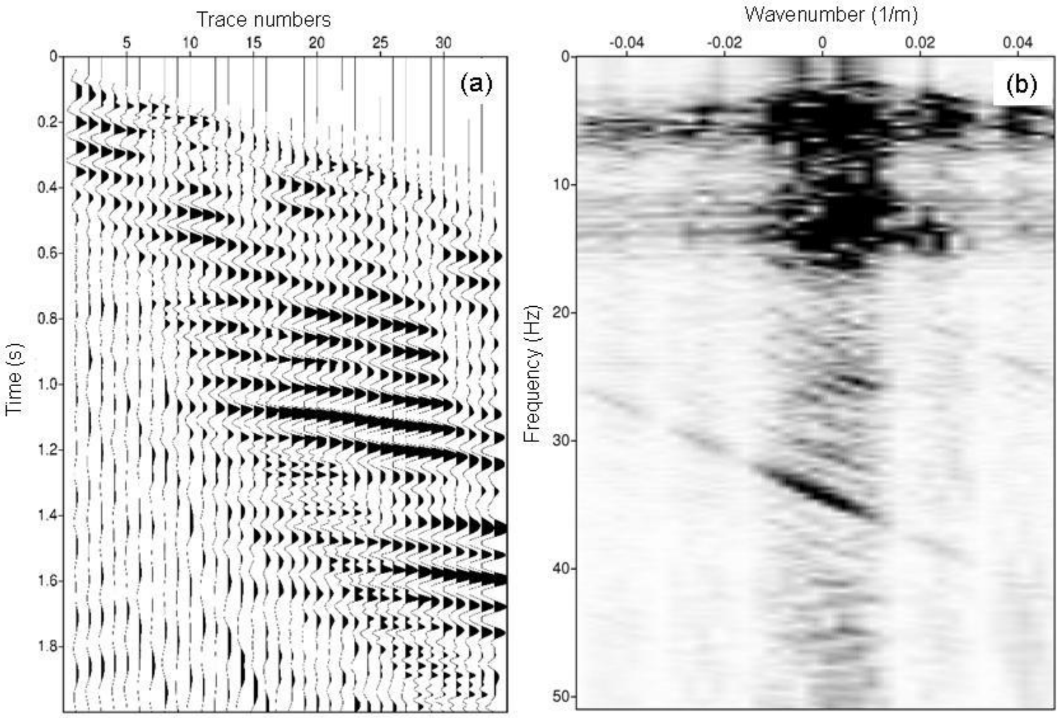

Fig. 19 – Linear array-response, trace spacing of 10 m, displayed in time (a) time and (b) frequency-wavenumber domain.

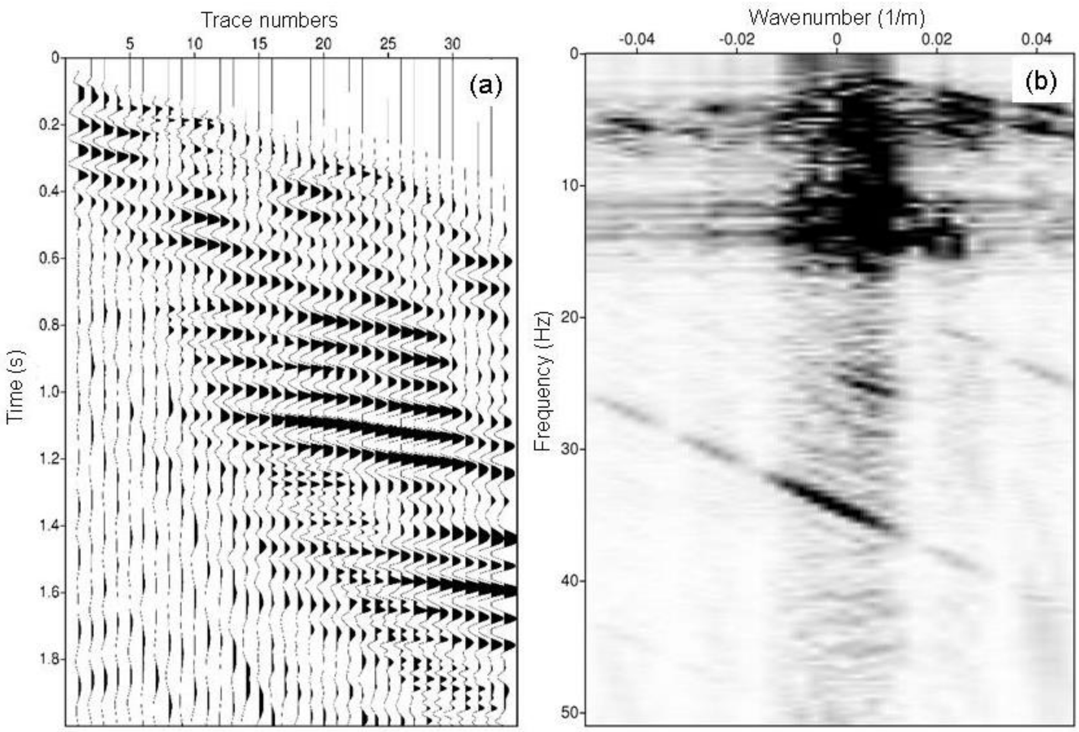

Fig. 20 – Rectangular array-response, trace spacing of 10 m, displayed in time (a) time and (b) frequency-wavenumber domain.

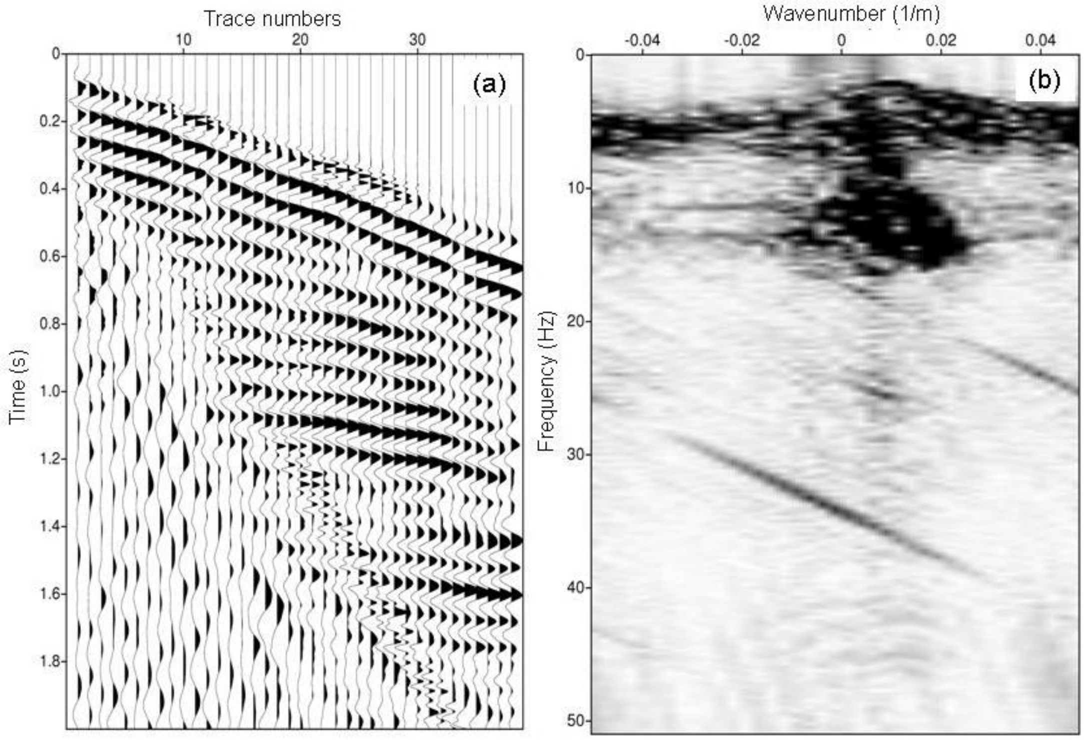

Fig. 21 – Circular array-response, trace spacing of 10 m, displayed in time (a) time and (b) frequency-wavenumber domain.

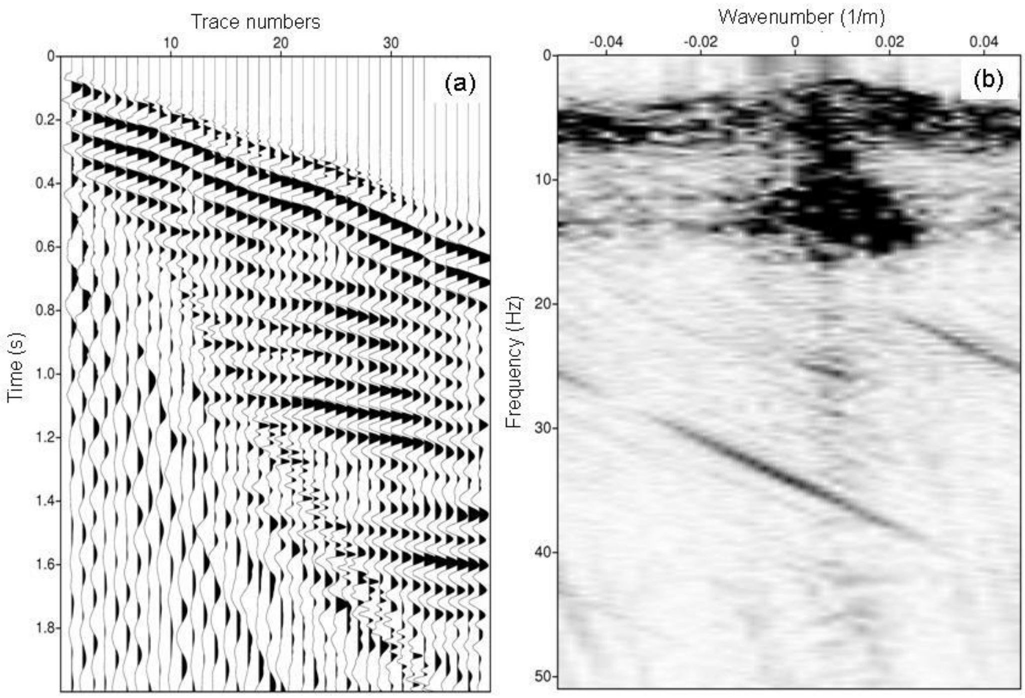

Fig. 22 – Cross array-response, trace spacing of 10 m, displayed in time (a) time and (b) frequency-wavenumber domain.

CONCLUSIONS

We compared the attenuation of the surface waves seen on single-sensor land seismic reflection data performed by linear and non-linear geophone arrays. The best attenuation was performed by the linear and rectangular arrays. Lowest surface wave attenuation was observed on the circular, cross and fishbone array-forming responses displayed in the (t, x)- and (f, k)-domains.

REFERENCES

PANEA, I. (2009), *Array forming in the presence of phase variations.* The Leading Edge, **28**, 2, pp. 216–221.

PANEA, I., DRIJKONINGEN, G. (2006), *Adaptive beamformers and time corrections.* Extended Abstract, EAGE Conf. Exhib., Vienna.

PANEA, I., DRIJKONINGEN, G. (2008), *The spatial data-adaptive minimum-variance distortionless-response beamformer on seismic single-sensor data.* Geophysics, **73**, 5, pp. Q29–Q42.

Received: February 7, 2018
Accepted for publication: October 22, 2018